Sonoelasticity of Organs:
Shear Waves Ring a Bell

Kevin J. Parker, PhD, Robert M. Lerner, MD, PhD

Sonoelasticity is the use of ultrasonography to visualize, in real time, the hardness or stiffness of tissues and organs by depicting the tissue's motion in response to an applied vibration source. The applied vibration source is usually of low amplitude and low frequency (less than 0.1 mm displacement and less than 2000 Hz). Under these conditions, the natural vibration response of tissues and whole organs is revealed as a standing wave pattern determined by the low-frequency elastic constants of the tissues and their boundary conditions, factors that are not related to the ultrasonic echogenicity. As a result, hard or dense isoechoic tumors that are undetectable by conventional ultrasonography often can be visualized in sonoelasticity imaging by virtue of their altered vibration response.

In this report, we demonstrate the appearance of organs such as the breast, liver, and kidney during real-time, in vivo sonoelasticity imaging. The results show that the shape and location of vibration patterns are dependent on the tissues and vibration frequencies; thus, information about the basic elastic properties of tissues should be obtainable. KEY WORDS: Doppler; Vibration; Palpation; Tumors; Elastic properties; Imaging; Tissue characterization; Sonoelasticity imaging.

The "stiffness" or "firmness" of tissues may be an important parameter in clinical evaluations. For example, cirrhosis of the liver can result in a palpably firm liver. However, none of the conventional medical imaging modalities are capable of assessing the basic elastic or mechanical properties of tissues that relate directly to the findings on clinical palpation. Ultrasonic echogenicity is related to the mechanical properties of tissues in the megahertz frequency range. Ultrasonography is dominated by longitudinal wave propagation because shear waves are rapidly attenuated at megahertz frequencies. Backscatter of ultrasound beams, and hence echogenicity of tissues, is related to the imaging frequency and distribution of impedence mismatches. Thus, echogenicity has little relationship to findings on clinical palpation (which is a low-frequency elastic phenomenon), under which circumstances we postulate that shear wave propagation dominates. Sonoelasticity has shown promise in phantom and in vitro studies that differentiate stiff focal regions from surrounding tissues.[1–6] In this report, we extend the work to preliminary results on whole organs in vivo.

VIBRATION ANALYSIS FOR TISSUES

A practical imaging device probably would not rely on analytic solutions to a fully posed boundary value problem as solved in the theory of vibrations in solids. However, insight into the experimental consequences and practical application of sonoelasticity imaging is provided by consideration of the theory of vibrations in solids. The detailed theory and solutions for the vibration patterns produced in a confined tissue specimen are beyond the scope of this work.[4,7] However, it is instructive to consider a simple example, as in the case of a rectangular solid of dimensions x_0, y_0, and z_0 cm, with given material properties such as density and Young's modulus (the viscous damping term is relevant

Received from the Rochester Center for Biomedical Ultrasound (K.J.P., R.M.L.), University of Rochester, and Rochester General Hospital (R.M.L.), Rochester, New York.

Address correspondence and reprint requests to Kevin J. Parker, PhD, Rochester Center for Biomedical Ultrasound, University of Rochester, Rochester, NY 14627.

We are grateful for the support of the University of Rochester Departments of Electrical Engineering and Radiology during a difficult funding era for "small science."

but not considered for brevity in this analysis).[7] The natural response or "eigen modes" of this structure includes simple sinusoidal vibration patterns in the x, y, and z directions. Examples of the simple and complicated modal shapes for an analogous two-dimensional clamped plate are shown in Figure 1. Simply put, vibration patterns range from a simple, lowest frequency pattern to higher frequency and more complicated natural vibration patterns. The natural vibration patterns of the elastic structure are eigenmodes or simply modal patterns, and the frequencies at which they occur are called eigenfrequencies. When the vibration source is applied at an eigenfrequency, efficient energy coupling to the tissue is realized and the vibrational velocities are high at the antinodes. For a lossless rectangular elastic solid with rigid boundaries, the eigenfrequencies occur only at specific frequencies:

$$f_{l,m,n} = \frac{c}{2}\sqrt{\left(\frac{l}{x^0}\right)^2 + \left(\frac{m}{y^0}\right)^2 + \left(\frac{n}{z^0}\right)^2}$$

where l, m, and n are integers (1, 2, 3, . . .) representing the mode number in the x, y, and z directions, respectively, and c is the speed of sound in the rectangular solid. It is important to note that C_l (longitudinal sound

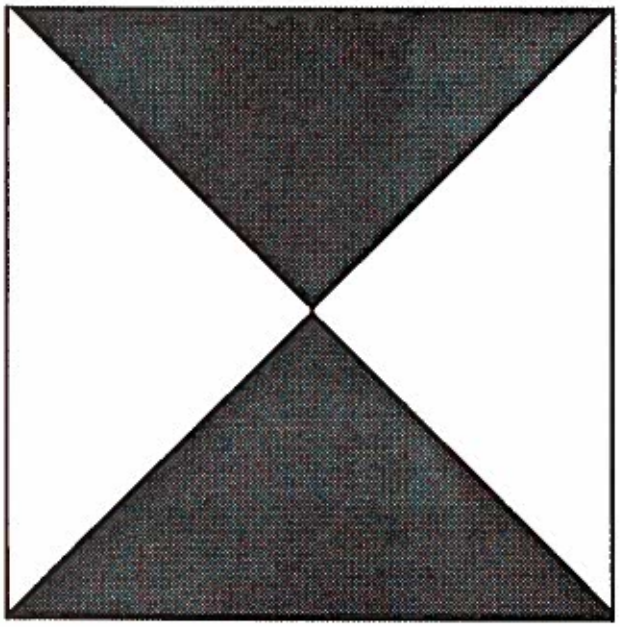

A

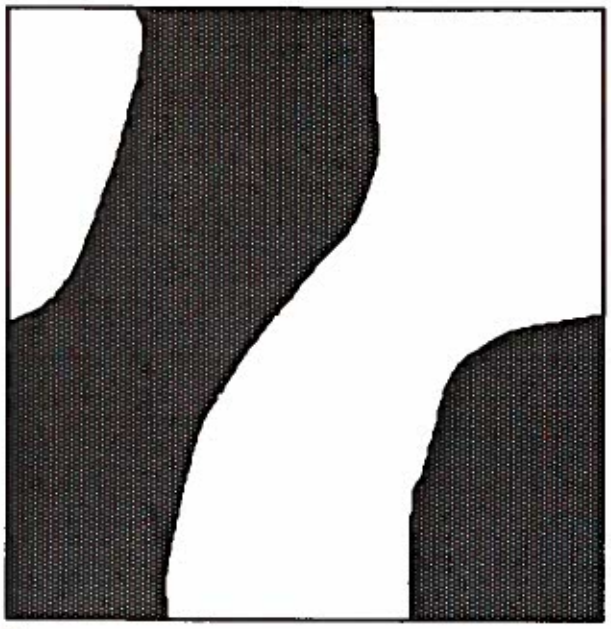

B

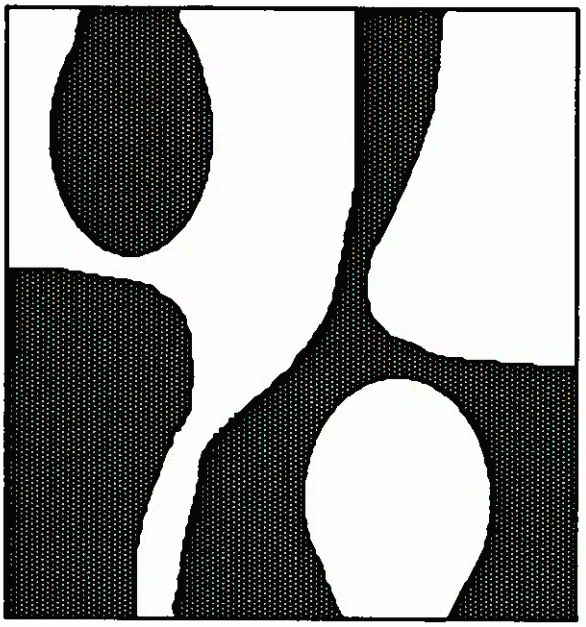

C

Figure 1 Modal patterns of clamped square plates indicate increasing complexity of vibration patterns for higher modes at higher frequencies. These results provide an analogy to the three-dimensional case. **A**, **B**, and **C** correspond to the fourth, seventh, and twelfth eiginmodes, respectively. (Adapted from Szilard R: Theory and Analysis of Plates. Englewood Cliffs, NJ, Prentice-Hall, 1975.)

speed) is considerably higher than C_s (shear wave sound speed) in biological tissues.[5]

As an example, consider a cube of tissue 9 cm on an edge, which is subjected to low-frequency vibrations in the 100 Hz regimen as in sonoelasticity. For a longitudinal wave speed of 1500 m/s, the wavelength for longitudinal wave propagation is 15 m at 100 Hz. This is clearly much larger than the size of the tissue, and even the fundamental resonant mode could not be established in a 9 cm cube. Shear wave speed, however, in tissue is of the order of 300 cm/s, and at 100 Hz excitation frequency the wave length for shear wave propagation[5] is of the order of 3 cm. Clearly, this is the appropriate size to set up standing wave patterns within a 9 cm block of tissue, and thus low-order resonance modes may be established.

Eigenmodes of solids can be excited by placing a small vibration source in contact with the solid and tuning the vibration frequency to a specific eigenfrequency. Figure 2A demonstrates an eigenmode pattern produced in a cubic homogeneous phantom. (In this example the top boundary is free and the others are constrained.) The effects of irregular boundaries and inhomogeneities is to distort the eigenmode pattern from what would be established in the case of a homogeneous, regular object. Figure 2B demonstrates a similar phantom as Figure 2A, excited at the similar frequency, except that phantom 2B also contains a soft, cube-shaped inclusion, which distorts the modal patterns. We have found that by examining the simpler, lower frequency modal patterns, inhomogeneities such as small, stiff tumors of the liver and prostate can be identified.[1–3,5,6] We emphasize in this report that the configuration of eigenmodes, visualized for the first time in sonoelasticity imaging, can reveal the mechanical properties (for example, shear wave speed) of an organ using equation 1 and other relations from the theory of solids. In this report we demonstrate what we believe are the first in vivo shear wave eigenmode patterns ever demonstrated.

METHODS FOR SONOELASTICITY IMAGING OF MODAL PATTERNS

Vibrations were coupled to in vitro specimens and live volunteers (all of whom gave informed consent) using an acoustic horn capable of output in the 20 to 1000 Hz audio band. The acoustic vibration source had a compliant 7 cm surface which was coupled by light pressure to the base of phantoms or the abdomen. Less than 10 watts of electrical power was input to the acoustic horn at all times, and the resulting vibrational amplitude at the point of contact was estimated to be less than 0.1 mm peak displacement at 200 Hz.

Images of the vibration patterns were made using a color Doppler instrument (*Quantum, QAD1*, Ipssequah, WA) at 7.5 and 5.0 MHz, as in our previous reports.[3,6] This instrument was adjusted to display vibration in a threshold mode. Saturated white and red overlays indicate regions where the vibrational amplitude exceeded some threshold dictated by the gain (signal level) and Doppler threshold controls. The presence or absence of color was not dependent on B-scan reflectivity over a reasonable (greater than 20 dB) range.

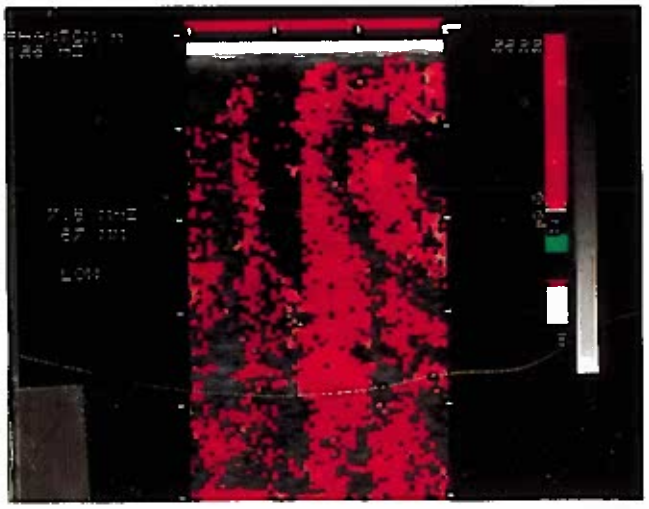

A

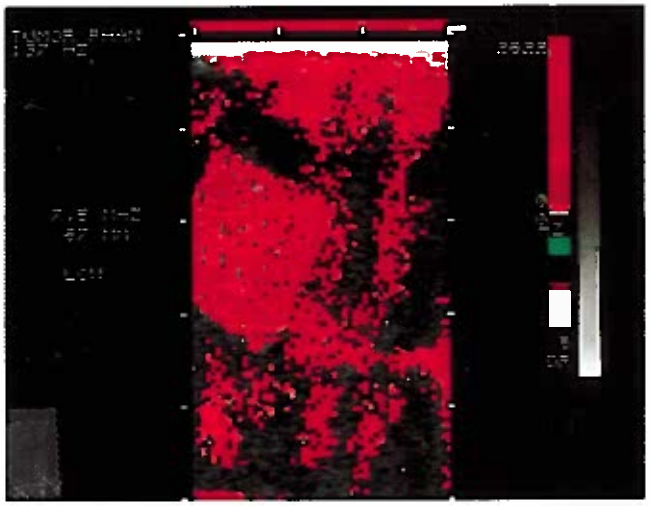

B

Figure 2 **A**, Sonoelasticity image (color Doppler vibration pattern) from a homogeneous agar phantom vibrated at 126 Hz and detected at 7.5 MHz using threshold configuration.[3] Saturated regions of red signify vibration above 0.05 mm in amplitude. Regions with less vibration are imaged in conventional gray scale. Complicated eigenmode pattern implies high-order mode (such as the twelfth mode of Fig. 1C). **B**, Sonoelasticity image (color Doppler vibration pattern) from agar phantom containing soft inclusion. External vibration at 137 Hz imaged at 7.5 MHz with color Doppler threshold configuration. The external vibration frequency was tuned to optimize coupling to the inclusion.

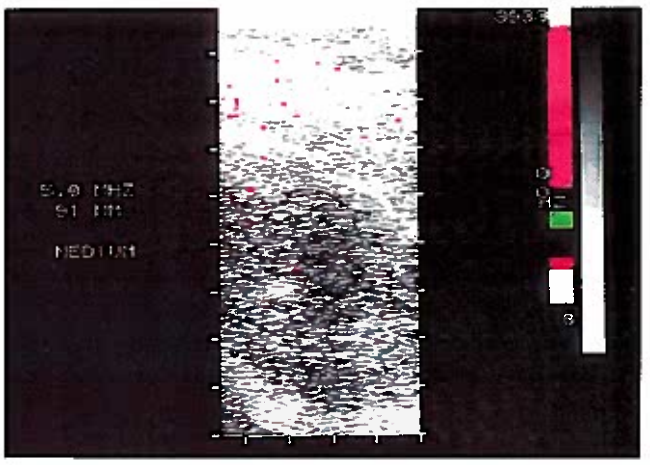

A

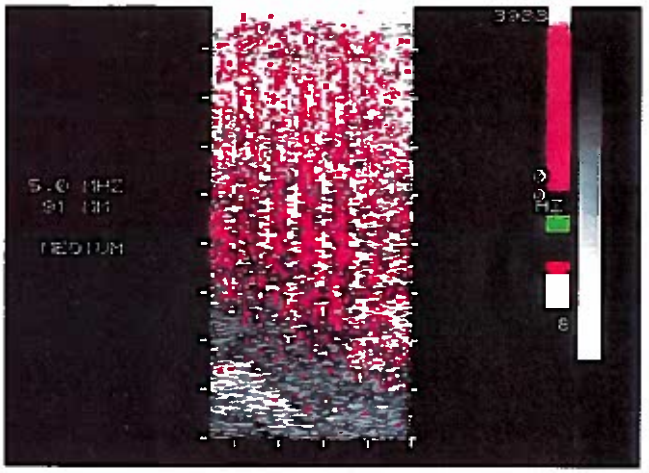

B

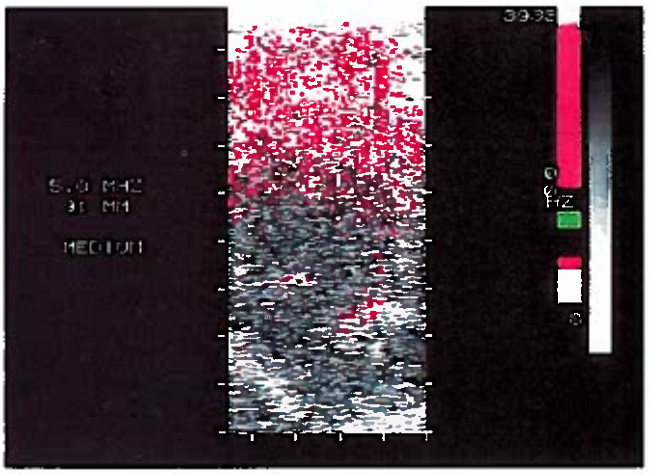

C

Figure 3 Sonoelasticity images of a normal right kidney imaged at 5 MHz from the posterior flank with a low-frequency vibration source on the anterior abdomen. **A**, Cross-section of kidney without vibration applied; random color dots represent background noise level. **B**, Sonoelasticity conditions same as in **A** with vibration source now on at approximately 100 Hz. Note high vibration velocities (antinodes) within the kidney and lower velocities in subcutaneous tissues posterior to kidney (*top*). Both red and white saturated bands indicate vibrations above threshold. (The change from red to white saturated regions is an artifact of the "beating" of the scanning rate against the vibration cycles.) **C**, Sonoelasticity conditions same as in **A** and **B** but with vibration source now 140 Hz. Note that subcutaneous vibration still persists, but not the large modal pattern within the kidney.

Thus, crude sonoelasticity images were obtained in which presence of color indicated detected vibration above a certain magnitude. In the results section, saturated red or white color regions represent the detection of approximately 0.05 mm vibration amplitude at 200 Hz. When vibration below threshold was present, the instrument displayed only conventional gray scale information.

Thus, modal patterns are visualized as regions of saturated color (corresponding to regions of peak vibrations) overlaid on the conventional B-scan images.

RESULTS AND DISCUSSION

Sonoelasticity imaging of a normal right kidney in vivo is depicted in Figure 3. The external vibration source was applied from the anterior abdominal wall with the color Doppler imaging transducer located over the volunteer's back. Figure 3A shows the color Doppler image with no source vibration applied. The random dots of color demonstrate the background noise level. Figure 3B was obtained with the same color Doppler instrument settings and the addition of an external frequency vibration (90 to 100 Hz) located on the anterior abdomen. Because the imaging transducer was placed over the posterior flank, anterior structures are at the bottom of the image, where no color is apparent. Instead, the bulk of the color fills in the middle to posterior aspect of the kidney. There is also fill-in of color to a less extent in the perinephric tissues extending posteriorly to the top of the image near the transducer face of the imaging system. With the vibration source in a fixed location and imaging parameters constant, the vibration frequency was varied and at 140 Hz, the pattern (Fig. 3C) showed a different mode, whereby no vibration was detected within the kidney and vibration was concentrated in the posterior perinephric tissues only. These patterns were reproducible and occurred abruptly with transitions in frequency. We observed a generalized preference for the higher vibration (antinode) or color to remain in the subcutaneous tissues and propagate around the subject at most frequencies, avoiding coupling to the internal organs except at specific frequencies as depicted.

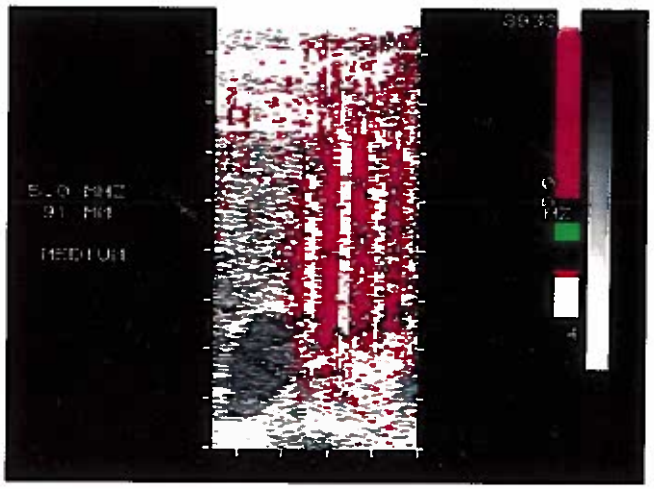

Figure 4 Sonoelasticity image of normal subject's liver imaged from the anterior abdominal wall with vibration source placed medial to it. The vibration frequency was adjusted to excite a vibrational mode in the liver. Note that the liver anterior to the gallbladder did not vibrate. The vibrational mode was confined to the liver and subcutaneous tissues. The right kidney posterior to the liver also did not vibrate at this frequency. The red and white alternating bands of color are an artifact of the sampling algorithm, but both indicate a region of vibration above threshold.

An in vivo sonoelasticity image from a normal liver is shown in Figure 4, with a single large mode of vibration within the liver resulting from a 100 Hz excitation source located near the abdominal midline. The visualizing transducer was located along the lateral abdominal wall over the liver. Multiple modes with complex structure were identified at higher frequencies. The lack of vibration overlying the gallbladder may be related to the changed boundary conditions of the pliable structure.

Sonoelasticity applied to a normal breast in vivo (Fig. 5) demonstrates that despite the complex different tissues within the breast (fat, fibrous tissues, blood vessels, and glands) modal patterns can be developed that change with frequency. Sonoelasticity from an in vitro surgical breast specimen (Fig. 6) shows a hypoechoic mass that is also identified by a sharp color boundary. High-level vibration is coupled to the subcutaneous and fatty tissue surrounding the glandular tissue, which appears as a lighter area with very little vibration on this modal image. The palpable mass was a malignant tumor that was stiffer than the adjacent glandular tissue, which showed limited but definite vibratory response.

The foregoing examples demonstrate that modal patterns of vibration can be demonstrated in vivo for a variety of tissues. We believe these patterns are for the most part related to shear wave propagation rather than longitudinal wave propagation.

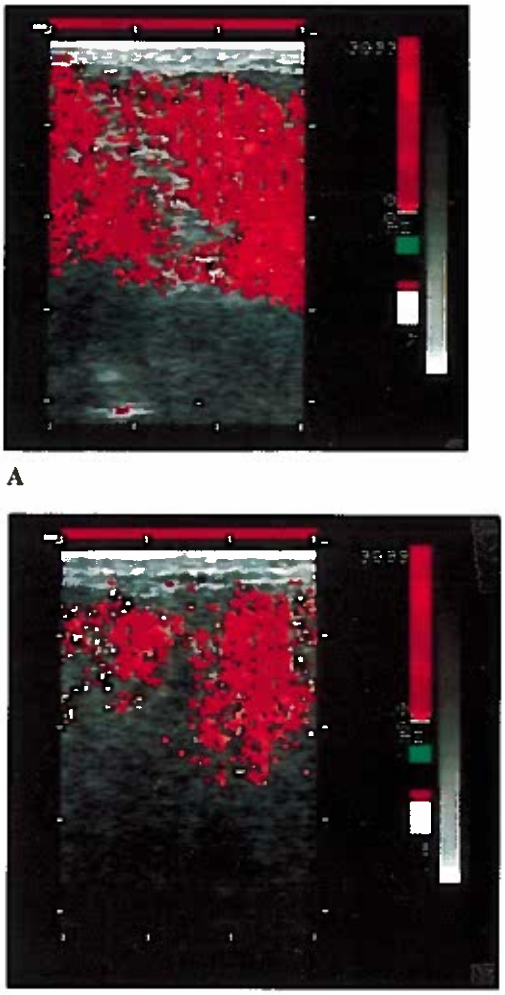

Figure 5 Sonoelasticity image of a normal subject's breast. **A, B,** A change in the modal pattern of color (vibration) is seen as a result of change in the low frequency.

Clearly, sonoelasticity is in its infancy. The images demonstrated here are bistable, or threshold images, and could be improved by implementing optimized time vibration estimators in a redesigned color imaging instrument.[8,9] In analogy to the development of conventional B-scan ultrasound, the leap from bistable to gray scale imaging brought a dramatic improvement in the clinical use of ultrasonography. Similarly, we expect substantial improvements in the usefulness of sonoelasticity as the imaging technology moves toward true graded vibration imaging. Nonetheless, our work to date demonstrates that, for the first time, eigenmodes or natural vibration patterns of whole organs can be visualized in real time, and this technique should provide new information concerning the in vivo elastic and material properties of tissue that are not obtainable by other means. The exciting work to be done will relate the low frequency mechanical prop-

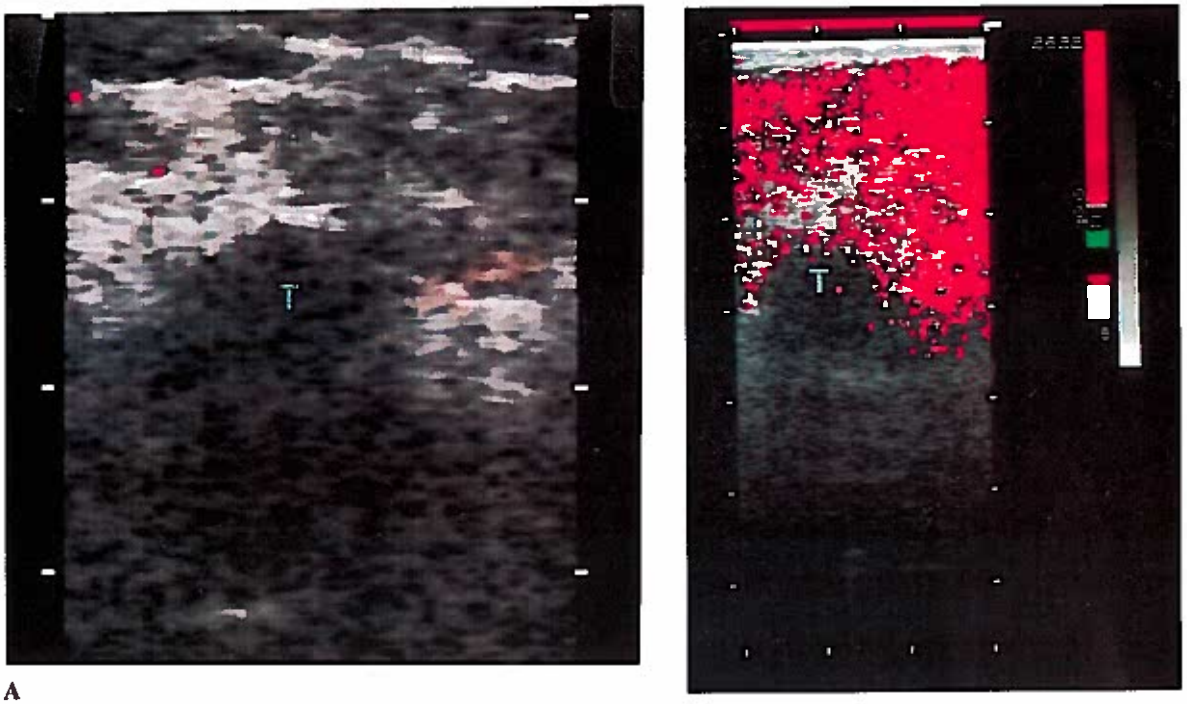

A B

Figure 6 Sonoelasticity image of an in vitro breast specimen from a patient with a palpable tumor. A, Color Doppler image (in "zoom" magnification) without low frequency vibration. B, Same configuration as in A but with low-frequency vibration applied (and without "zoom"—that is, under normal magnification). Palpable tumor (t) excluded vibration to a greater extent than overlying normal breast tissue, which showed limited motion. Surrounding subcutaneous fat showed enhanced vibration at these experimental conditions.

erties to the vibration patterns demonstrated in phantoms and in vivo studies.

REFERENCES

1. Lerner RM, Parker KJ: Sonoelasticity images derived from ultrasound signals in mechanically vibrated targets. *In* Thjissen, J (ed): Ultrasonic Tissue Characteristics and Echographic Imaging 7. Proceedings of the 7th European Communities Workshop, Nijmegen, Netherlands, 1987
2. Lerner RM, Parker KJ, Holen J, et al: Sonoelasticity: Medical elasticity images derived from ultrasound signals in mechanically vibrated targets. Acoust Imaging 16:317, 1988
3. Lerner RM, Huang S, Musulin R, et al: Sonoelasticity images derived from ultrasound signals in mechanically vibrated tissues. Ultrasound Med Biol 16:231, 1990
4. Parker KJ, Huang S, Musulin R, et al: Tissue response to mechanical vibrations for sonoelasticity imaging. Ultrasound Med Biol 16:241, 1990
5. Huang SR: Principles of sonoelasticity imaging and its applications in hard tumor detection. PhD Thesis, Department of Electrical Engineering, University of Rochester, New York, 1990
6. Lee F Jr, Bronson JP, Lerner RM, et al: Sonoelasticity imaging: Results in in vitro tissue specimens. Radiology 181:237, 1991
7. Szilard R: Theory and Analysis of Plates. Englewood Cliffs, NJ, Prentice Hall, 1975
8. Huang SR, Lerner RM, Parker KJ: On estimating the amplitude of harmonic vibration from the Doppler spectrum of reflected signals. J Acoust Soc Am 88: 2702, 1990
9. Huang SR, Lerner RM, Parker KJ: Time domain Doppler estimators of the amplitude of vibrating targets. J Acoust Soc Am 91: 965, 1992